2019

Metabolic engineering of *Escherichia coli* for the *de novo* stereospecific biosynthesis of 1,2-propanediol through lactic acid

Wei Niu

Levi Kramer

Joshua Mueller

Kun Liu

Jiantao Guo

Metabolic Engineering Communications 7 (2018) e00082

Contents lists available at ScienceDirect

Metabolic Engineering Communications

journal homepage: www.elsevier.com/locate/mec

Metabolic engineering of *Escherichia coli* for the *de novo* stereospecific biosynthesis of 1,2-propanediol through lactic acid

Wei Niu[a,*], Levi Kramer[a], Joshua Mueller[a], Kun Liu[b], Jiantao Guo[b]

[a] *Department of Chemical & Biomolecular Engineering, University of Nebraska-Lincoln, Lincoln, NE 68588, United States*
[b] *Department of Chemistry, University of Nebraska-Lincoln, Lincoln, NE 68588, United States*

ARTICLE INFO

Keywords:
1,2-propanediol
Lactic acid
Reduction
Stereospecific
Escherichia coli

ABSTRACT

1,2-propanediol (1,2-PDO) is an industrial chemical with a broad range of applications, such as the production of alkyd and unsaturated polyester resins. It is currently produced as a racemic mixture from nonrenewable petroleum-based feedstocks. We have reported a novel artificial pathway for the biosynthesis of 1,2-PDO via lactic acid isomers as the intermediates. The pathway circumvents the cytotoxicity issue caused by methylglyoxal intermediate in the naturally existing pathway. Successful *E. coli* bioconversion of lactic acid to 1,2-PDO was shown in previous report. Here, we demonstrated the engineering of *E. coli* host strains for the *de novo* biosynthesis of 1,2-PDO through this pathway. Under fermenter-controlled conditions, the *R*-1,2-PDO was produced at 17.3 g/L with a molar yield of 42.2% from glucose, while the *S*-isomer was produced at 9.3 g/L with a molar yield of 23.2%. The optical purities of the two isomers were 97.5% *ee* (*R*) and 99.3% *ee* (*S*), respectively. To the best of our knowledge, these are the highest titers of 1,2-PDO biosynthesized by either natural producer or engineered microbial strains that are published in peer-reviewed journals.

1. Introduction

Microbial strains are rich sources of catalytic activities that enable both in vitro and in vivo biosyntheses of useful molecules at high titer, yield, and quite often, with superior stereoselectivity from a variety of renewable carbon sources, including lignocellulosic materials and CO_2 (Sheldon, 2014; Lee et al., 2012; Nielsen and Keasling, 2016). The biosynthetic power of a single microbe is further expanded when enzymes with promiscuous substrate specificity are exposed to molecular species that share the same functional group and similar carbon skeleton to their native substrates. Synthetic pathways can therefore be devised by combining enzymatic activities from different biological sources into a single host strain in order to achieve the synthesis of target molecules that are not endogenous metabolites or are not even natural products (Weeks and Chang, 2011; Niu et al., 2016; Chatsurachai et al., 2012; Campodonico et al., 2014; Niu et al., 2003; Yim et al., 2011). Moreover, synthetic pathways are also explored for natural products in order to provide ingenious solutions to engineering problems that are intrinsic to naturally existing routes (Atsumi et al., 2008; Bogorad et al., 2013).

1,2-Propanediol (1,2-PDO) is a commodity chemical with an annual global consumption of over 1.5 million metric tons and annual global market value of $2.7 billion in 2007 (Shelley, 2007). It is an intermediate in the production of alkyd resins for paints and high-performance, unsaturated polyester resins. It is also the preferred ingredient in coolant and deicing agent over ethylene glycol, due to its low melting point and low toxicity. Because of its Generally Recognized As Safe (GRAS) status, 1,2-PDO of pharmaceutical grade is widely used as co-solvent for low water-soluble compounds in drug and food formulation (Forkner et al., 2005). Current industrial production of 1,2-PDO racemic mixture is mainly through high pressure, high temperature, noncatalytic hydrolysis of propylene oxide, which is a building block derived from non-renewable petroleum resources (Forkner et al., 2005). Renewable synthesis of 1,2-PDO through microbial catalysis has been studied for decades (Shelley, 2007). As a natural product, accumulation of 1,2-PDO was first reported in the culture of *Clostridium thermobutylicum* (Lennart, 1954). The biosynthetic pathway (Fig. 1b) was later delineated (Cameron and Cooney, 1986) and engineered into *E. coli* hosts for 1,2-PDO synthesis from glucose and glycerol (Altaras and Cameron, 2000; Clomburg and Gonzalez, 2011). The best titer of 4.9 g/L (0.19 g/g) and 5.6 g/L (0.21 g/g) was achieved when glucose and glycerol was provided as the carbon source, respectively (Clomburg and Gonzalez, 2011). None of the engineered strains was able to outperform the natural producer *C. thermosaccharolyticum*, which produced 1,2-PDO at a final titer of 9.0 g/L (0.2 g/g) from glucose (Sanchez-Riera et al., 1987). One major

* Corresponding author.
E-mail address: wniu2@unl.edu (W. Niu).

https://doi.org/10.1016/j.mec.2018.e00082
Received 13 June 2018; Received in revised form 19 November 2018; Accepted 19 November 2018

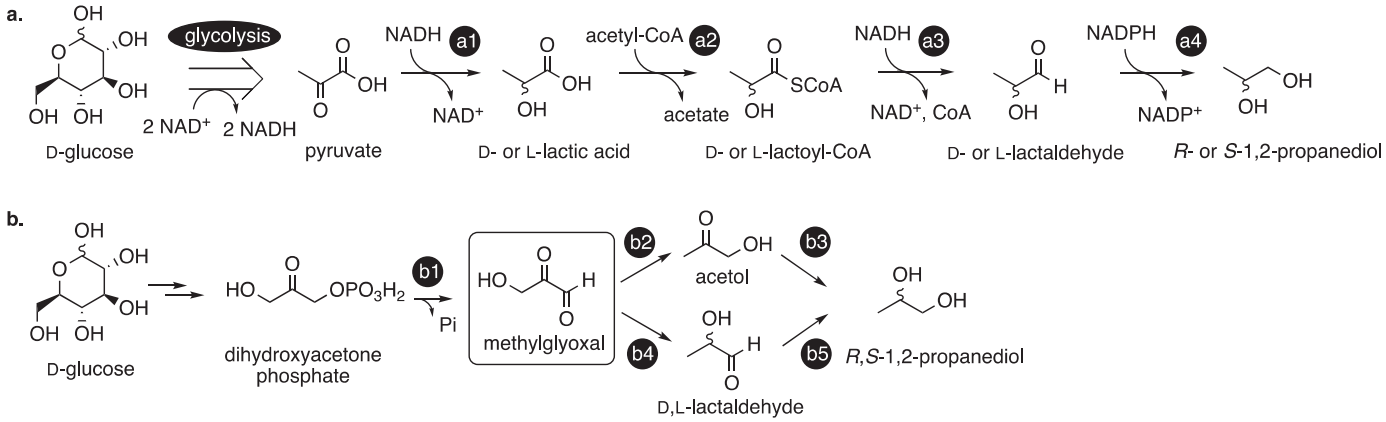

Fig. 1. Biosynthetic pathways of 1,2-PDO. a. Artificial pathway. (a1) lactate dehydrogenase (*ldhA* or *lldh*); (a2) lactoyl-CoA transferase (*pct*); (a3) CoA-dependent aldehyde dehydrogenase (*pduP*); (a4) lactaldehyde reductase (*yahK*). **b.** Natural pathway. (b1) methylglyoxal synthase; (b2) aldehyde oxidoreductase; (b3) glycerol dehydrogenase; (b4) methylglyoxal reductase; (b5) 1,2-propanediol reductase.

obstacle in the engineering of the natural 1,2-PDO pathway lies in the cytotoxicity inflicted by the obligate biosynthetic intermediate methylglyoxal at submillimolar concentrations (Fig. 1b) (Totemeyer et al., 1998; Booth et al., 2003). To circumvent this problem, we have previously designed a synthetic 1,2-PDO pathway in which the common fermentation product, lactic acid, was chosen as the branching point of 1,2-PDO synthesis from *E. coli* fermentative metabolism (Fig. 1a) (Niu and Guo, 2015). In addition to the elimination of methylglyoxal as an intermediate, the synthetic pathway can potentially enable the exclusive accumulation of the *R*- or the *S*-1,2-PDO stereoisomer from the D- or the L-lactic acid intermediates. In this report, we present the engineering strategy of *E. coli* hosts that enabled the *de novo* biosynthesis of 1,2-PDO directly from glucose as the carbon source. We examined culturing conditions and genetic manipulations to optimize the flux into the 1,2-PDO pathway. Under fed-batch fermentation conditions, engineered *E. coli* strains produced 1,2-PDO stereoisomers of high optical purity at final concentrations of 17.3 g/L (*R*-) and 9.3 g/L (*S*-), respectively.

2. Materials and methods

2.1. General methods

All commercial chemicals are of reagent grade or higher. Acetyl-CoA, sodium D-lactate, sodium L-lactate, NADH, and NADPH were purchased from Sigma. All solutions were prepared in deionized water that was further treated by Barnstead Nanopure® ultrapure water purification system (Thermo Fisher Scientific Inc). Bacterial strains constructed and used in this study are listed in Table 1. LB medium (1 L) contained Bacto tryptone (10 g), Bacto yeast extract (5 g), and NaCl (10 g). M9 salts (1 L) contained Na_2HPO_4 (6 g), KH_2PO_4 (3 g), NH_4Cl (1 g), and NaCl (0.5 g). M9 glucose medium contained glucose (10 g), $MgSO_4$ (0.12 g), $CaCl_2$ (0.028 g) and thiamine hydrochloride (0.001 g) in 1 L of M9 salts. Fed-batch fermentation media (850 mL) contained Na_2HPO_4 (6.78 g), KH_2PO_4 (3 g), NH_4Cl (2 g), NaCl (0.5 g) and $(NH_4)_2SO_4$ (1 g). Antibiotics were added where appropriate to the following final concentrations: chloramphenicol (in methanol), 17 mg/L; kanamycin, 50 mg/L; ampicillin, 100 mg/L. Isopropyl-*β*-D-thiogalactopyranoside (IPTG) was prepared as a 100 mM stock solution. Solutions of M9 salts, glucose, $MgSO_4$, and $CaCl_2$ were autoclaved separately and then mixed. Solutions of antibiotics, IPTG, and thiamine hydrochloride were filtered through 0.22 μm sterile membrane filters.

Table 1
Bacterial strains and plasmids used in the study.

strain/plasmid	characteristics	source
MG1655	wild-type K12	CGSC 6300[a]
Δ^3	MG1655, Δ*adhE*, Δ*dld*, Δ*lldD*	21
Δ^7	Δ^3, Δ*frdA*, Δ*pflB*, Δ*mgsA*, Δ*aldA*	this study
Δ^8	Δ^7, Δ*arcA*	this study
Δ^8 *lldh*	Δ^8, replaced the *ldhA* gene with the *lldh* gene	this study
Pediococcus acidilactici	wild-type	DSMZ 20284
2.094	Cm^R, *yahK* in pSU18	21[b]
2.096	Ap^R, *pduP* and *pct* in pJF118EH	21[c]

[a] CGSC, Coli Genetic Stock Center, http://cgsc2.biology.yale.edu.
[b] renamed from pWN2.094; [c.] renamed from pWN2.096-yahK.

Standard protocols were used for the construction, purification, and analysis of plasmid DNA (Sambrook et al., 2000). Bacterial genomic DNAs were isolated using the PureLink™ genomic DNA mini kit (Life Technologies). PCR amplifications were carried out using KOD HotStart DNA polymerase by following manufacturer's protocol. Restriction endonucleases were purchased from New England Biolabs. Electroporation was performed with Electroporator 2510 (Eppendorf AG). Primer synthesis and DNA sequencing services were provided by Eurofins MWG Operon. Primers used in this study are listed in Table 1S.

2.2. Analytical methods

Concentrations of accumulated metabolites in culture medium were quantified by ^{1}H NMR. Samples of fermentation broth were centrifuged to obtain cell-free broth, which was subsequently mixed with D_2O at a 9:1 (v/v) ratio. The sodium salt of 3-(trimethylsilyl)propionic-2,2,3,3-d_4 acid (TSP) was included in the D_2O at a known concentration as the internal standard for calibration and quantification purpose. All ^{1}H NMR spectra were recorded on a Bruker Avance III-HD NMR Spectrometer (300 MHz). A solvent suppression program was applied to suppress the signal of water. Concentrations were determined by comparison of integrals corresponding to each compound with the integral corresponding to TSP (δ = 0.00 ppm). A standard concentration curve was determined for each metabolite of interest. Compounds were quantified using following resonance signals: 1,2-PDO (δ 1.12, d, 3H); ethanol (δ 1.20, t, 3H); lactate (δ 1.35, d, 3H); alanine (δ 1.50, d, 3H); acetate (δ 1.94, s, 3H); pyruvate (δ 2.38, s, 3H); glucose (δ 3.25, t, 1H (β)). The enantiomeric purity of 1,2-PDO was analyzed following a previously reported method (Niu and Guo, 2015).

2.3. Enzyme assays

Enzyme assays were conducted using cell-free lysate. Cells were collected by centrifugation followed by the removal of supernatant. Harvested cells were lysed using BugBuster® protein extraction reagent

(EMD Millipore). The cell-free lysate was obtained by centrifugation at 21,300*g* for 30 min at 4 °C. Activities of the lactoyl-CoA transferase, lactoyl-CoA dehydrogenase, and lactaldehyde reductase were determined by following previously reported methods (Niu and Guo, 2015). Lactate dehydrogenase activities were determined by measuring the pyruvate-dependent oxidation of NADH at 37 °C (Zhou et al., 2003a). Protein concentrations were determined using the Bio-Rad protein assay kit (Bio-Rad Laboratories). Biotek Synergy H1 hybrid platereader was used to record absorbance changes.

2.4. Host strain construction

A previously constructed *E. coli* strain Δ^3 was used as the initial parent strain in this study (Niu and Guo, 2015). A two-step scarless chromosomal modification method was carried out using the λ Red-mediated recombineering method (Zhang et al., 1998; Sharan et al., 2009) for the sequential deletion of *E. coli* genes *frdA*, *pflB*, *mgsA*, *aldA*, *arcA* and the replacement of *ldhA* gene (encodes D-lactate dehydrogenase) with the *Pediococcus acidilactici lldh* gene (encodes L-lactate dehydrogenase). The *sacB*-encoded *Bacillus subtilis* levansucrase was used as the counterselection marker (Edwards et al., 1998). The genotypes of all candidate strains were confirmed by DNA sequencing of the modified sites.

2.5. Batch fermentation

Single colony of an *E. coli* strain was introduced into 5 mL of LB media containing appropriate antibiotics. The seed culture was cultivated at 37 °C for 12 h with shaking. A 0.5 mL aliquot of the seed culture was transferred into 9.5 mL of freshly prepared M9 glucose media with appropriate antibiotics and IPTG (0.25 mM) in a 12 mL serum vial. The vial was then flushed with N_2, capped with a rubber stopper and aluminum cap, and sealed using a crimper. The anaerobic culture was cultivated at 37 °C with shaking for 72 h. To achieve micro-aerobic cultivation conditions, a 21 G needle was inserted into the rubber stopper to allow the diffusion of air into the sealed vials. Batch fermentations were run in triplicate. Results were reported as the average of the three runs.

2.6. Fed-batch fermentation

Fed-batch fermentations were carried out in a 2-L working volume BIOSTAT® B bioreactors (Sartorius Stedim Biotech). Temperature and pH were controlled with proportional-integral-derivative (PID) control loops. The temperature was maintained at 37 °C. The pH was controlled at 7.0 by the addition of acid (2 N H_2SO_4) and base solutions (concentrated NH_4OH at the aerobic stage or 20% $NaHCO_3$ at the micro-aerobic stage). Dissolved oxygen was measured using an OxyFerm probe. A seed culture was started by the introduction of a single colony into 5 mL of M9 glucose medium. Culture was grown at 37 °C with shaking for 16 h and subsequently transferred into 95 mL of M9 glucose medium. The culture was grown under the same conditions for an additional 10 h. A fermentation was initiated by transferring the seed culture (100 mL) into the fermentation vessel, which contained the fed-batch fermentation medium (850 mL) and 20 g of glucose (50 mL). The total initial volume of the fermentation culture was 1 L. A two-stage cultivation scheme was used. The first stage took approximately 8 h. At the first stage, the D.O. was maintained at 10% air saturation through sequential ramping of impeller speed and airflow rate to the preset values. At this point, the $OD_{600\,nm}$ reached approximately 10. Expression of the 1,2-PDO pathway was induced by IPTG at a final concentration of 0.25 mM. Following an additional 1 h of cultivation, the microaerobic stage was initiated by reducing the airflow rate to 20 cm^3 per minute (ccm). This was defined as t = 0 h in the fed-batch fermentations. At the same time, 100 g of glucose in solution (600 g/L) was fed into the fermenter at a constant rate over 24 h. Throughout the second stage, the D.O. value registered as 0.0% air saturation. Appropriate antibiotics were included at every culturing stage. Fed-batch fermentations were run in triplicate. Results were reported as the average of three runs.

2.7. In silico simulation

The *in silico* simulation was performed by using the *E. coli* genome-scale metabolic model iML1515 (Monk et al., 2017) consisting of 2719 metabolic reactions and 1192 unique metabolites in the COnstraint-Based Reconstruction and Analysis Toolbox v2.0 (COBRA toolbox) (Schellenberger et al., 2011). The model was modified to enable the synthetic pathway of lactic acid to 1,2-PDO conversion. In addition to the gene-protein-reaction relationship (GPR) for the three reactions catalyzed by enzymes Pct, PduP, and YahK, a transport reaction for the export of 1,2-PDO was also included. Constraint-based flux analysis was performed on strains derived from the rationally engineered host Δ^7, in which genes *dld*, *lldD*, *adhE*, *frdA*, *pflB*, *mgsA*, and *aldA* were deleted. To implement the gene deletion during the *in silico* simulation, fluxes through the corresponding reactions were set to zero. The Flux Variability Analysis (FVA) (Mahadevan and Schilling, 2003) was performed using the built-in function of COBRA toolbox (Schellenberger et al., 2011).

3. Results

3.1. Construction of E. coli host for the accumulation of D-lactic acid

To enable the *de novo* biosynthesis of 1,2-PDO from sugar substrate, we first took a rational approach to design an *E. coli* host. Since lactate is the direct precursor of 1,2-PDO biosynthesis in our previously reported synthetic pathway, we initially targeted the construction of an *E. coli* host that is capable of homolactate fermentation based on literature reports (Zhou et al., 2003b; Wang et al., 2012). Genes encoding enzymes in fermentative production of ethanol (*adhE*), succinate (*frdA*), and formate (*pflB*) were deleted from the genome of *E. coli* K-12 parent MG1655 in order to eliminate competing pathways that can lead to the accumulation of byproducts. To prevent possible backflux from lactate to pyruvate, the *dld* and *lldD* genes, which encode two membrane-associated lactate dehydrogenases, were also deleted. Our previous report showed that an *E. coli* strain was able to convert lactate stereoisomers into 1,2-PDO stereoisomers with virtually no loss of optical purity (Niu and Guo, 2015). To explore the potential of stereospecific *de novo* biosynthesis, we also eliminated genes that contribute to possible stereo-center scrambling. Since the optical purity of 1,2-PDO directly relies on the optical purity of lactate, the methylglyoxal bypass, which was identified to be the source of racemization in lactate fermentation (Grabar et al., 2006), was inactivated through the deletion of methylglyoxal synthase encoding gene (*mgsA*). The *aldA* gene, which encodes a broad substrate specificity aldehyde dehydrogenase, was also deleted to lead to strain Δ^7. Removal of the AldA activity benefits the 1,2-PDO biosynthesis through the minimization of the backflux from lactaldehyde to lactate.

Strain Δ^7 was first evaluated for its ability to accumulate D-lactic acid under anaerobic growth condition in sealed serum vials. Cells were cultured in M9 minimal medium with glucose as the sole carbon source. To avoid perturbation to the culturing condition, a single sample was taken at 72 h. The cell density reached an $OD_{600\,nm}$ of 1.5, while 47.8 ± 1.2 mM of lactate was accumulated in a 147.0 ± 3.7% (mol/mol) yield. Besides lactate, a low concentration of acetate (1.3 ± 0.2 mM) was the only other detectable metabolite in ^1H NMR analysis. The yield of lactate synthesized by Δ^7 is comparable to previously reported *E. coli* strain cultured under similar conditions (Chang et al., 1999).

Table 2
Cell growth and metabolite accumulation of serum vial experiments.

	Δ^7		Δ^8		Δ^8 lldh	
	anaerobic	**micro-aerobic**	**anaerobic**	**micro-aerobic**	**anaerobic**	**micro-aerobic**
$OD_{600\,nm}$	1.5 ± 0.1	1.9 ± 0.1	1.4 ± 0.1	1.9 ± 0.1	0.8 ± 0.1	1.0 ± 0.1
1,2-PDO	4.2 ± 0.4	7.0 ± 1.1	5.5 ± 0.2	10.1 ± 0.7	0.5 ± 0.1	4.0 ± 0.1
lactate	48.5 ± 0.9	42.3 ± 1.0	47.7 ± 0.9	40.5 ± 0.9	11.4 ± 3.3	8.6 ± 3.4
ethanol	0.9 ± 0.1	2.4 ± 0.5	1.4 ± 0.1	3.1 ± 0.7	0.31 ± 0.1	2.8 ± 0.1
acetate	1.5 ± 0.2	15.1 ± 2.2	3.1 ± 0.5	17.3 ± 2.0	0.7 ± 0.1	17.6 ± 1.8
PDO yield	11.8 ± 1.0	16.9 ± 2.9	14.5 ± 1.0	22.3 ± 1.8	4.5 ± 0.2	12.5 ± 0.3
(PDO+lactate) yield	146.8 ± 4.0	118.4 ± 5.4	144.7 ± 3.6	111.6 ± 4.1	105.1 ± 6.8	38.4 ± 6.9

* Each host was transformed with plasmids 2.094 and 2.096. Data was collected 72 h after the inoculation. The metabolite concentrations are in mM. The yields are expressed as % (mol of metabolite per mol of glucose). The data are the average of three independent trials.

3.2. De novo biosynthesis of R-1,2-PDO via D-lactate

The lactate to 1,2-PDO segment of the synthetic pathway was installed in strain Δ^7 by transforming the host cells with two previously constructed plasmids, 2.094 and 2.096 (Niu and Guo, 2015). Plasmid 2.094 contains a gene cassette of *pduP* and *pct*, which encodes the lactoyl-CoA dehydrogenase and the CoA transferase, respectively. Plasmid 2.096 encodes the lactaldehyde reductase (*yahK*). The transcription of genes on both plasmids was controlled through the lac operators embedded in the promoter. A plasmid-borne copy of the *lacI* gene resides on 2.094 to enable stringent control of the gene expression. The resulting strain was first examined under anaerobic conditions in serum vials (column 1, Table 2). Following 72 h of cultivation, 1,2-PDO was accumulated at 4.2 ± 0.4 mM with a yield of 11.8 ± 1.0% (mol/mol) from glucose. Other metabolites, including lactate (48.5 ± 0.9 mM), acetate (1.5 ± 0.2 mM) and ethanol (0.9 ± 0.1 mM), were also observed. The combined yield of 1,2-PDO and lactate was 146.8 ± 4.0%, which is similar to the lactate yield of the host strain Δ^7. Deletion of the *adhE* eliminated the ethanol production by Δ^7 when the host itself was cultured under the anaerobic condition. Ethanol produced by strain in Δ^7/2.094/2.096 is likely due to the introduction of the 1,2-PDO pathway. In particular, the promiscuous reduction activity of the PduP enzyme on acetyl-CoA led to the formation of acetaldehyde, which can be further reduced to form ethanol (Niu and Guo, 2015).

The anaerobic synthesis of lactate through glycolysis from glucose by *E. coli* is a pathway with perfect balance between the generation and the consumption of the reducing equivalents, while the conversion from lactate to 1,2-PDO constitutes two additional reduction steps. In addition, the PduP enzyme, which functions at the first reduction step from lactate to 1,2-PDO (Fig. 1a), has poor kinetics on the nonnative substrate, lactoyl-CoA (Niu and Guo, 2015). Insufficient supply of NADH/NADPH can therefore lead to accumulation of lactate and low titer and yield of 1,2-PDO under the anaerobic condition as observed above. To this end, we further explored whether changes in culturing conditions can improve the titer and yield of 1,2-PDO. Since higher NADH per glucose yield can be achieved through the oxidative branch of the TCA cycle in the presence of oxygen, strain Δ^7/2.094/2.096 was then examined under microaerobic growth condition in serum vials (column 2, Table 2). Following 72 h of cultivation, 1,2-PDO was produced at an elevated titer of 7.0 ± 1.1 mM and an improved yield of 16.9 ± 2.9% (mol/mol). Change of culturing condition also resulted in acetate at a tenfold higher concentration and more ethanol in the media. Although increased biomass was observed under the microaerobic conditions, the strain produced more 1,2-PDO per cell (3.7 mM/OD_{600}) than that under the anaerobic conditions (2.8 mM/OD_{600}). Since similar activities of pathway enzymes were observed regardless of the availability of oxygen (data not shown), change of cellular metabolism is likely the reason for the improvement. Meanwhile, despite the increased titer and yield of 1,2-PDO, a roughly 20% reduction in the combined yield of lactate and 1,2-PDO was observed, which is likely the result of losing pyruvate to cell mass and respiration.

3.3. Optimization of R-1,2-PDO biosynthesis

Engineered *E. coli* host Δ^7 provides the entry point to *de novo* biosynthesis of 1,2-PDO from glucose. However, an engineered homolactate-producing strain cannot satisfy the redox requirement to achieve the maximum titer and yield of 1,2-PDO biosynthesis under anaerobic growth. The maximum theoretical yield of 1,2-PDO from glucose is calculated to be 1.5 mol/mol under the non-growth condition. To identify enabling genetic manipulations, we performed *in silico* simulation using the modified *E. coli* genome-scale model iML1515 (Monk et al., 2017) that included deletions in host strain Δ^7 and the 1,2-PDO biosynthetic pathway. By setting the biomass production as the objective function, Flux Variability Analysis (FVA) shows that flux through 1,2-PDO biosynthesis varied between arbitrary values of 0–0.153 (mmol/gCDW/h). Comparison of the flux distributions revealed a small flux through the pyruvate dehydrogenase into the TCA cycle that led to the increased yield of 1,2-PDO. In addition, the yield of lactate was predicted to decrease, while the yields of acetate and CO_2 should increase. Since the reactions of pyruvate dehydrogenase and TCA cycle afford additional redox molecules, *in silico* simulation indicated a viable strategy to increase the availability of NAD(P)H for 1,2-PDO biosynthesis.

We next sought to engineer an *E. coli* host that has a partially active TCA cycle when grown under microaerobic conditions. This was achieved by the construction of an *E. coli* Δ^8 strain through the deletion of *arcA* gene from the Δ^7 strain. The ArcA protein is a global transcriptional regulator. Together with membrane-associated kinase, ArcB, ArcA regulates the expression of respiratory and fermentative pathways (Lynch and Lin, 1996). Under anaerobic condition, ArcA serves as a repressor protein for the expression of enzymes functioning in the oxidative branch of the TCA cycle. The strategy of ArcA deletion to enable microaerobic carbon flux into the TCA cycle has been successfully implemented in the engineering of 1,4-butanediol-producing *E. coli* (Yim et al., 2011). Strain Δ^8 was first evaluated for lactate accumulation in sealed serum bottle under anaerobic conditions. After 72 h, Δ^8 behaved similarly as strain Δ^7 in biomass production ($OD_{600\,nm}$ = 1.6), accumulation of lactate (47.7 ± 0.3 mM, in 146.9 ± 1.0% (mol/mol) yield) and acetate (1.9 ± 0.2 mM). The major difference was that Δ^8 strain also produced a small amount of succinate (1.4 ± 0.1 mM).

The capability of host Δ^8 to support 1,2-PDO biosynthesis was then evaluated using strain Δ^8/2.094/2.096 in serum vials. Under the anaerobic condition (columns 3, Table 2), this strain accumulated higher concentration and yield of 1,2-PDO in comparison to Δ^7/2.094/2.096. Reduced lactate and increased acetate accumulations were also observed. Above behaviors are consistent with the simulation results. Similar to the observation when host Δ^7 was used, the 1,2-PDO titer

under the microaerobic condition (column 4, Table 2) was higher than that under the anaerobic condition (column 3, Table 2). In the meantime, a lower concentration of lactate was observed for the Δ^8 strain when low level of O_2 was available, which also led to a reduced combined yield of PDO and lactate. A small amount of succinate (1.0 ± 0.1 mM) was only observed under the anaerobic condition (data not included in Table 2). Above data showed that the ArcA deletion strategy succeeded in improving the biosynthesis of 1,2-PDO.

3.4. S-1,2-PDO biosynthesis in L-lactate-producing E. coli host

A major benefit of our artificial 1,2-PDO biosynthetic pathway is the facile production of the *R*- or *S*- stereoisomer by switching between the D- and the L-lactate biosynthetic precursors (Fig. 1a). To enable the *de novo* biosynthesis of *S*-1,2-PDO, *E. coli* host Δ^8 lldh was constructed by replacing the endogenous *ldhA* gene with the *lldh* gene from *Pediococcus acidilactici* (Zhou et al., 2003a). Strain Δ^8 lldh was first evaluated for lactate accumulation in serum vials under anaerobic conditions. An $OD_{600\ nm}$ value of 0.8 was reached, which is only around 50% of the cell density achieved by the two engineered D-lactate-producing hosts, Δ^7 and Δ^8. Lowered concentrations of lactate (32.0 ± 2.2 mM, in 130.0 ± 5.9% (mol/mol) yield) were produced. In addition to acetate (2.4 ± 0.1 mM), the strain accumulated other C3 metabolites including pyruvate (3.2 ± 0.3 mM) and alanine (1.2 ± 0.1 mM). Succinate was not observed in the culture medium. Both pyruvate and alanine are not common fermentation products of *E. coli*. Their accumulations were interpreted as the result of insufficient lactate dehydrogenase activities. The hypothesis was supported by the observation of reduced lactate production, albeit of similar combined yield of C3 compounds (147.9 ± 10.6%, mol/mol) to those of the D-lactate producing hosts. To test this hypothesis, enzyme assays of lactate dehydrogenase were performed using cell lysate of *E. coli* Δ^7, Δ^8, and Δ^8 lldh that were cultured under the same anaerobic conditions (Fig. 2). Similar activities (around 0.1 U/mg) were observed in the two strains (Δ^7 and Δ^8) that expressed the native D-lactate dehydrogenase. However, the L-lactate dehydrogenase activity cannot be unambiguously detected in the cell lysate of Δ^8 lldh, due to background activities of other NADH oxidizing enzymes.

1,2-PDO accumulation by strain Δ^8 lldh/2.094/2.096 was tested in serum vials. Under anaerobic condition, the cell growth reached similar density as when the host strain was cultured. Both lactate (11.4 ± 3.3 mM) and 1,2-PDO (0.5 ± 0.1 mM) was accumulated at reduced concentrations and yields in comparison to those by strain Δ^8/2.094/2.096 (column 5, Table 2). The same trend of reduced cell growth, titer and yield of lactate and 1,2-PDO was also observed when limited oxygen was available (column 6, Table 2). The accumulations of both pyruvate and alanine were observed as well (data not shown).

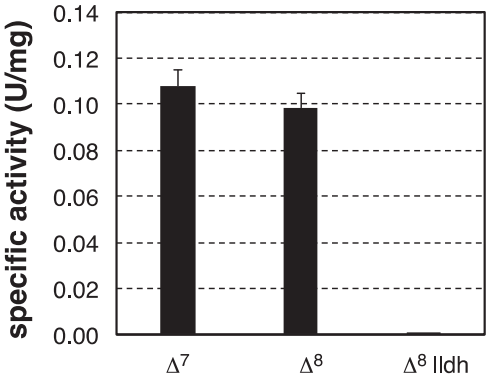

Fig. 2. The lactate dehydrogenase activities of *E. coli* hosts. One unit of enzyme activity is defined as the oxidation of 1 μmol of NADH in one minute at 37 °C. The data is the average of three measurements. The error bars indicate the standard deviation.

3.5. De novo biosynthesis of 1,2-PDO stereoisomers under fermenter-controlled conditions

The biosynthesis of *R*-1,2-PDO by strains Δ^7/2.094/2.096 and Δ^8/2.094/2.096 was further examined and compared under fermenter-controlled cultivation conditions. To achieve higher titer and yield, a two-stage cultivation scheme was implemented. At the first stage, the cells were grown under aerobic condition in order to accumulate cell mass and shorten the overall process time. The expression of the plasmid-encoded pathway enzymes was induced 1 h prior to the transition into the second cultivation stage, during which limited amount of air (20 ccm) was sparged into the culture vessel with a stirring rate of 560 rpm. Fermentation was continued under the microaerobic condition for an additional 24 h while glucose was fed to the cells at a constant rate. Cell density, metabolite accumulations, and activities of pathway enzymes (Fig. S1) were analyzed at indicated time points. The cell growth occurred mainly at the first stage. A similar growth profile was observed for the two strains (Table S2). A roughly 15% increase in cell density was observed in the first 4 h after the initiation of the second stage (Fig. 3A and C). For the Δ^7-derived strain, *R*-1,2-PDO was produced at a relatively consistent rate of around 2.7 mmol/L/h (0.2 g/L/h) to reach the final titer of 65.8 mM (5 g/L) and yield of 12.4% (mol/mol). For the Δ^8-derived strain, a higher volumetric productivity of *R*-1,2-PDO at around 5.5 mmol/L/h (0.4 g/L/h) was achieved, which was accompanied by a higher final titer (131.8 mM, 10 g/L) and higher yield (24.9%, mol/mol). Besides *R*-1,2-PDO, lactate was the major byproduct accumulated by both strains, although a higher titer of *R*-1,2-PDO by Δ^8 strain led to a slightly reduced accumulation of lactate (452 mM, 40.8 g/L, 86.0% (mol/mol)) in comparison to that of Δ^7 strain (466 mM, 42.0 g/L at 88.5% (mol/mol)). Another major difference between the two strains was the drastically reduced acetate accumulation in the absence of ArcA expression. A 25.7% reduction in acetate production was observed for strain Δ^8/2.094/2.096 (115.2 mM) in comparison to strain Δ^7/2.094/2.096 (155 mM). Other minor metabolites, including ethanol, pyruvate and alanine, were observed at similar concentrations at every time point for both strains (Fig. 3B and D).

The biosynthesis of *S*-1,2-PDO by strain Δ^8lldh/2.094/2.096 was examined under the same fermenter-controlled cultivation conditions. At the aerobic stage, no growth defect was observed (Table S2). The result indicates that the low biomass production by Δ^8 lldh strains under limited availability of oxygen is likely caused by the inefficient recycling of redox molecules due to low lactate dehydrogenase activities. Without this limitation, the *S*-1,2-PDO-producing construct grew similarly as its *R*-1,2-PDO-producing counterpart (Table S2). At the second microaerobic stage, the two strains also showed very similar growth and 1,2-PDO production profiles (Fig. 3C and E). The Δ^8 lldh construct reached a volumetric productivity of *S*-1,2-PDO at 5.1 mmol/L/h (0.37 g/L/h), a final titer of 122.6 mM (9.3 g/L) and a yield at 23.2% (mol/mol), which were comparable to the values of the Δ^8 construct. However the accumulation profiles of lactate and other metabolites by the two strains were drastically different (Fig. 3D and F). Instead of lactate (121.1 mM), pyruvate (205.2 mM) was accumulated as the major biosynthetic intermediate by the Δ^8 lldh strain. The final concentration of acetate was further reduced by almost twofold, while concentrations of alanine and ethanol increased.

To further explore the effect of aeration on the biosynthesis of 1,2-PDO stereoisomers under the fermenter-controlled conditions, strains Δ^8/2.094/2.096 and Δ^8lldh/2.094/2.096 were evaluated using the same cultivation scheme as above but with lowered stirring rate at 280 rpm in the second stage. The two strains showed similar growth profiles, where the cell density constantly declined at the microaerobic stage of the cultivation (Fig. 4A and C). In comparison to fermentations with stirring rate of 560 rpm, lowered aeration led to increased accumulation of *R*-1,2-PDO by strain Δ^8/2.094/2.096 (227.9 mM, 17.3 g/L) at higher yield and productivity (42.2% (mol/mol), 0.72 g/

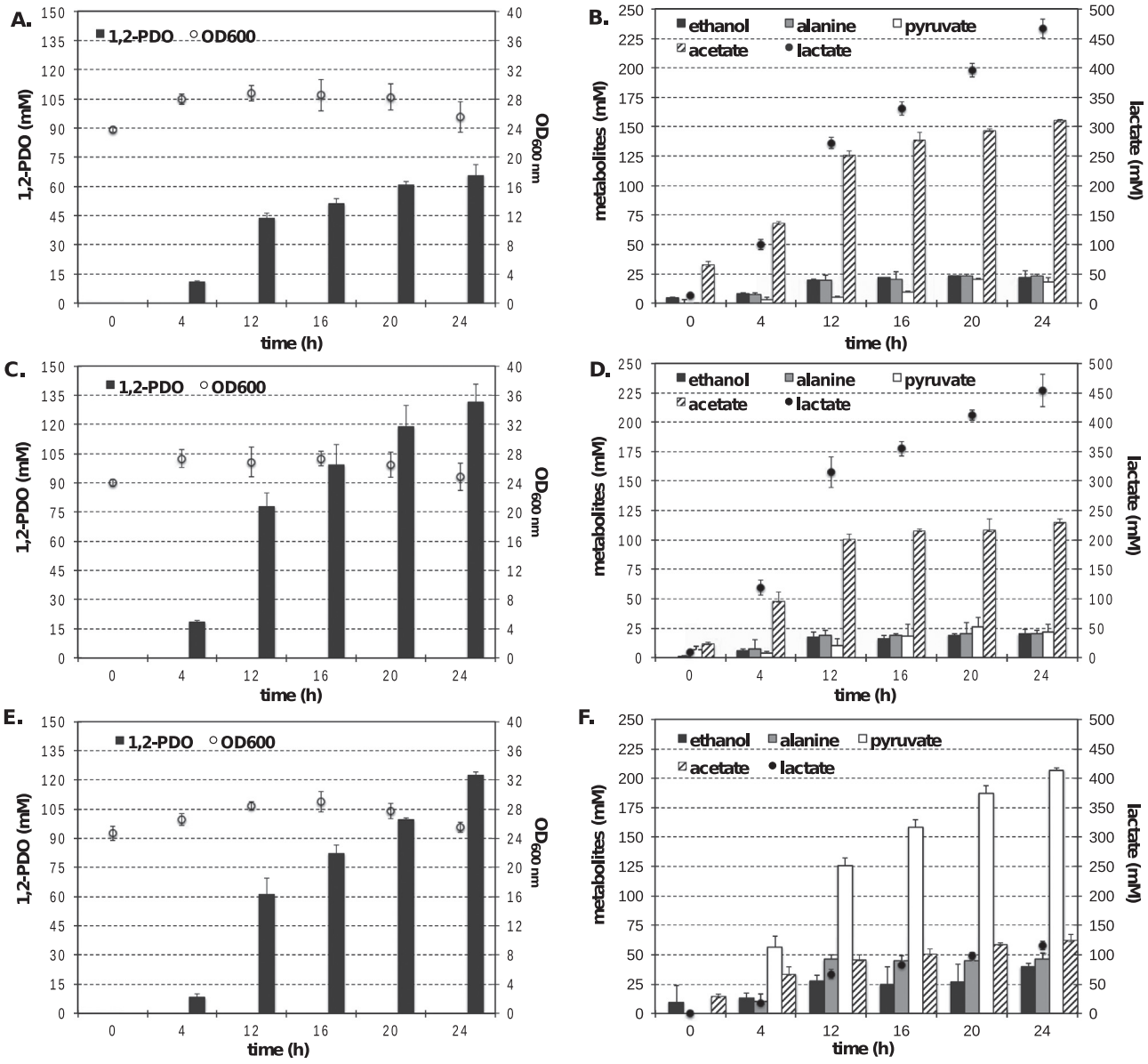

Fig. 3. Biosynthesis of *R*-1,2-PDO and *S*-1,2-PDO by *E. coli* strains under fermenter-controlled conditions (560 rpm stirring rate). A. Time courses of cell growth and 1,2-PDO concentrations of Δ^7/2.094/2.096. B. Time courses of metabolite accumulations of Δ^7/2.094/2.096. C. Time courses of cell growth and 1,2-PDO concentrations of Δ^8/2.094/2.096. D. Time courses of metabolite accumulations of Δ^8/2.094/2.096. E. Time courses of cell growth and 1,2-PDO concentrations of Δ^8lldh/2.094/2.096. F. Time courses of metabolite accumulations of Δ^8lldh/2.094/2.096. The data is the average of three fermentation runs. The error bars indicate the standard deviation.

L/h) (Fig. 4A) and reduced accumulations of lactate (380.7 mM, 34.3 g/L, 69.4% (mol/mol)) and other metabolites, including acetate, pyruvate, and alanine (Fig. 4B). An opposite trend of metabolite accumulation was observed for strain Δ^8lldh/2.094/2.096, which showed poor glucose uptake at the microaerobic stage of the cultivation (Fig. S2). As the result, *S*-1,2-PDO was synthesized at a final concentration of 18.6 mM (1.4 g/L, 11.3% (mol/mol)) (Fig. 4C), which represents an approximate 85% reduction from conditions with higher stirring rate. Pathway intermediates (pyruvate and lactate) and all byproducts were also produced at low concentrations (Fig. 4D).

To confirm the stereospecificity of the *de novo* biosynthesis, 1,2-PDO from fermentations of both the Δ^8 and Δ^8 lldh constructs were subjected to optical purity analysis (Fig. 5). Enantiomeric excess of 97.5% and 99.3% were observed for the *R*- and the *S*- isomer, respectively.

4. Discussion and conclusions

Implementation of designed synthetic pathways to expand the metabolic and catalytic diversity of platform host strains provides great opportunities to find straightforward solutions to challenging metabolic engineering problems. Addition of a limited number of biochemical reactions to a well-studied metabolic network extends the product profile of the host. In the meantime, host engineering benefits from readily available knowledge of cell physiology and genetic tools. To circumvent a highly cytotoxic biosynthetic intermediate in a naturally existing 1,2-PDO biosynthetic pathway, we published an initial study to demonstrate the feasibility of direct conversion of lactate stereoisomers into corresponding 1,2-PDO isomers (Niu and Guo, 2015). The current study further established the entire pathway in *E. coli* host strains to achieve the *de novo* and stereospecific biosynthesis of 1,2-PDO isomers using glucose as the carbon source. Because lactic acid fermentation by *E. coli* strain was well-established, initial strain engineering was focused on the deletion of competing pathways

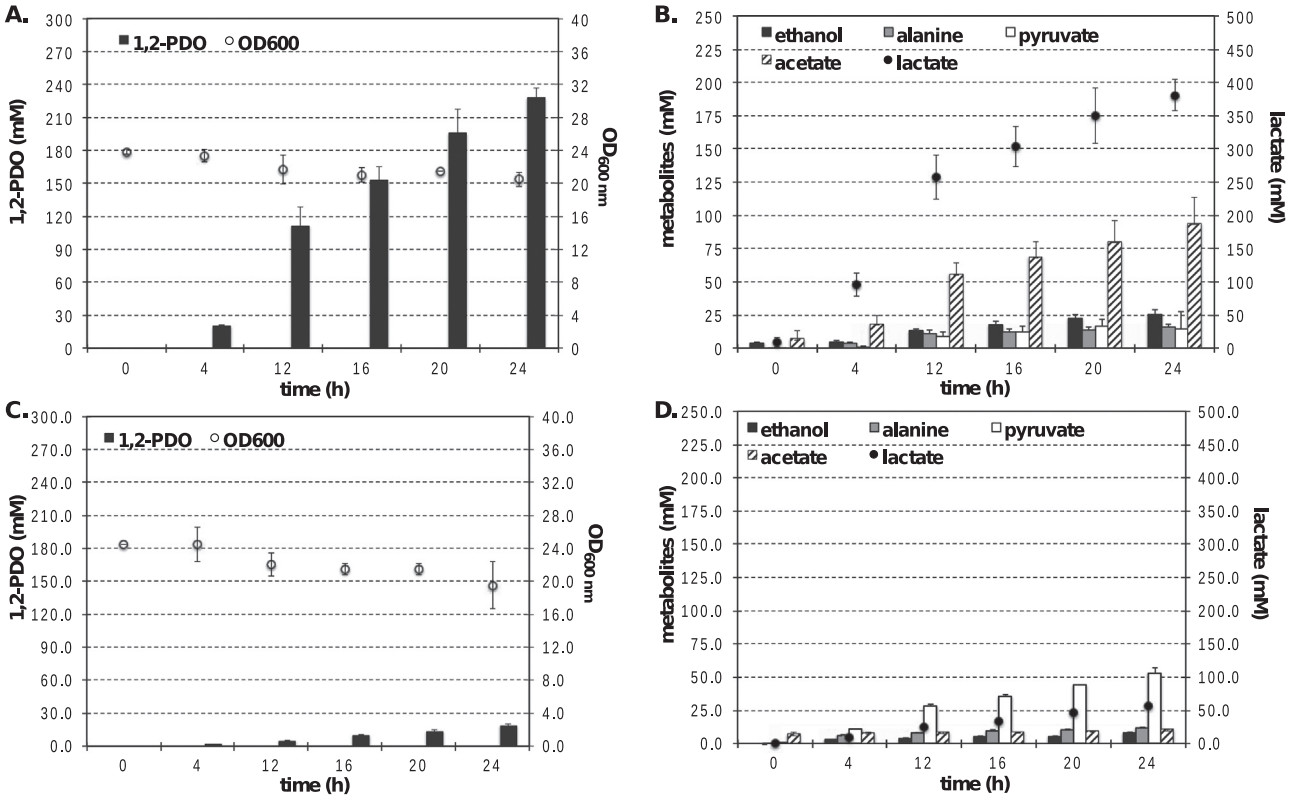

Fig. 4. Biosynthesis of *R*-1,2-PDO and *S*-1,2-PDO by *E. coli* strains under fermenter-controlled conditions (280 rpm stirring rate). A. Time courses of cell growth and 1,2-PDO concentrations of Δ^8/2.094/2.096. B. Time courses of metabolite accumulations of Δ^8/2.094/2.096. C. Time courses of cell growth and 1,2-PDO concentrations of Δ^8 lldh/2.094/2.096. D. Time courses of metabolite accumulations of Δ^8 lldh/2.094/2.096. The data is the average of three fermentation runs. The error bars indicate the standard deviation.

and the elimination of possible backflux routes, which led to a strain that produced *R*-1,2-PDO at 4.2 mM under anaerobic and 7.0 mM under microaerobic conditions in serum vials. Although a higher cell density was reached with increased availability of oxygen, the increased titer cannot be completely attributed to the increased biomass production, due to the increased yield and cell productivity, 3.7 vs. 2.7 (mM per $OD600_{nm}$). We argued that increased availability of reducing equivalents, which is key in engineering a highly efficient 1,2-PDO producer, played a major role. By applying simulation using *in silico* model, we identified the control of the flux into the TCA cycle as a viable route of overproducing NAD(P)H. Elimination of the regulatory protein ArcA in above host further improved the yield and titer of 1,2-PDO under both the anaerobic and microaerobic conditions. The strategy was further confirmed to be effective when the Δ^7 and Δ^8 derived strains were examined under fermenter-controlled, two-stage cultivation conditions. The titer, yield and volumetric productivity of *R*-1,2-PDO all showed a nearly twofold increase in the deregulated strain.

Additional insights into the synthetic pathway and the engineered strains were obtained when the behaviors of strain Δ^8/2.094/2.096 (producer of *R*-isomer) and strain Δ^8lldh/2.094/2.096 (producer of *S*-isomer) were examined under fermenter-controlled cultivation conditions (Table 3). At a stirring rate of 560 rpm, strain Δ^8 showed moderate growth in the first 12 h of cultivation followed by a slow decline of cell density at the microaerobic stage. At a stirring rate of 280 rpm, continuous decrease of cell density was observed. Since aeration is the only variable that was changed, the results indicate that the oxygen transfer rate at low stirring rate is not sufficient to sustain the initial high cell density resulting from the aerobic stage of the cultivation. This condition of reduced oxygen availability led to increased titer and yield of *R*-1,2-PDO by the Δ^8 strain, while the combined yield of all C3 metabolites stays similar to that of the condition of higher aeration (Table 3). The observation demonstrates that to improve the availability of intracellular redox molecules by controlling the aerobic respiration is still a viable strategy for strains with deregulated microaerobic metabolism via the *arcA* deletion. Systematic optimization of the fermentation process will be explored to further improve the *R*-1,2-PDO biosynthesis. Unlike the observation in serum vials, the Δ^8lldh strain did not show different biomass profile

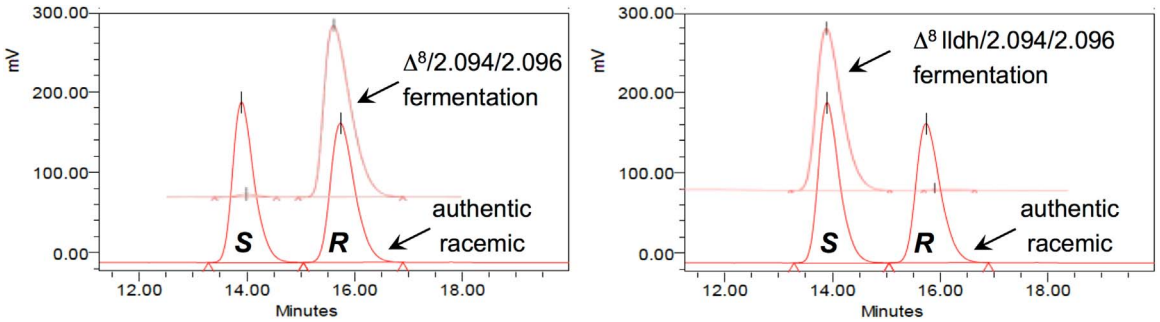

Fig. 5. Enantiomeric purity analysis of microbial synthesized 1,2-PDO isomers.

Table 3
Summary of fermentation yields.

yield[b] (%, mol/mol)	Δ^7 strain[a] 560 rpm	Δ^8 strain 560 rpm	Δ^8 lldh strain 560 rpm	Δ^8 strain 280 rpm	Δ^8 lldh strain 280 rpm
1,2-PDO	12.4 ± 1.1	24.9 ± 2.8	23.2 ± 1.0	42.2 ± 1.3	11.3 ± 0.8
lactate	88.0 ± 5.0	86.0 ± 4.1	21.4 ± 0.7	69.4 ± 1.2	34.8 ± 0.5
pyruvate	3.5 ± 0.5	4.6 ± 1.2	37.8 ± 1.6	1.8 ± 0.3	35.4 ± 1.5
alanine	4.4 ± 0.4	3.7 ± 0.6	8.5 ± 0.8	2.9 ± 0.2	7.1 ± 0.2
C3 combined	108.3 ± 5.0	119.2 ± 4.1	89.7 ± 1.6	116.2 ± 1.3	88.6 ± 1.5

[a] Each strain contains plasmids 2.094 and 2.096.
[b] The data is the average of three fermentation runs. The error bars indicate the standard deviation.

from that of Δ^8 strain at the microaerobic stage. The strain also produced similar titer and yield of 1,2-PDO as the Δ^8 strain at the stirring rate of 560 rpm. Based on the undetectable L-lactate dehydrogenase activity (Fig. S1) and our hypothesis that growth of Δ^8 lldh cell was limited by the turnover of redox molecules when oxygen is limited, the results indicate that cell growth and 1,2-PDO synthesis is not coupled at the second stage of fermentation under this condition. It is more likely that the *S*-1,2-PDO biosynthesis is mainly controlled by the kinetics of the pathway enzymes. One intriguing result is the altered ratio between pathway intermediates and the final product. The molar ratio of pyruvate: lactate:1,2-PDO of Δ^8 strain was roughly 0.24:3.4:1 at 24 h, while the value changed to 1.7:0.94:1 for Δ^8 lldh strain. The reduced lactate dehydrogenase activities in the Δ^8lldh strain could benefit the subsequent reduction steps through presumably increased availability of reducing equivalents. On the other hand, when the stirring rate was reduced to 280 rpm, the Δ^8lldh strain showed drastically reduced metabolic activity, which led to glucose accumulation and low titers of all metabolites, including the product, *S*-1,2-PDO. The different behavior between Δ^8 and Δ^8lldh strains under the reduced aeration condition pinpoints the strategy for further optimization of *S*-1,2-PDO biosynthesis is to increase the kinetics of the L-lactate biosynthesis reaction.

A hypothetical two-step conversion via the intermediacy of lactaldehyde was first proposed for the observed reduction of lactate into 1,2-PDO by anaerobic cultures of *Lactobacillus buchneri* strains (Elferink et al., 2001). However, the genetic elements of the process are still unknown. A two-enzyme cascade consisting of a carboxylic acid reductase (CAR) and a lactaldehyde reductase was recently constructed to mimic the proposed two-step pathway, albeit with low efficiency due to poor kinetics of CAR on lactate substrates (Kramer et al., 2018). In this report, metabolic engineering strategies were successfully devised and applied to the construction of *E. coli* hosts for the stereospecific *de novo* biosynthesis of 1,2-PDO isomers through the reduction of lactate via a three-enzymes pathway (Fig. 1a). To the best of our knowledge, these engineered strains achieved the highest titer of 1,2-PDO stereoisomers with high optical purity in comparison to published results in peer-reviewed journals. The current yield of *R*-1,2-PDO biosynthesis is only about 28% of the maximum theoretical yield, while *S*-1,2-PDO biosynthesis is only about 16%. In addition to aforementioned approaches, such as process optimization, we perceive that further improvement lies in successfully identifying and implementing strategies to further increase the availability of redox molecules and/or optimizing the kinetics of pathway enzymes.

Acknowledgements

This work was supported by Grant CBET 1438332 (to W.N. and J.G.) from NSF. The funder had no role in study design, data collection and analysis, decision to publish, or preparation of the manuscript. The authors would like to acknowledge assistance from the following individuals at the University of Nebraska-Lincoln: Prof. David Berkowitz (Department of Chemistry, chiral HPLC), Dr. Martha Morton (Department of Chemistry, ^{1}H NMR), Mr. Howard Willett (Department of Chemical and Biomolecular Engineering, ^{1}H NMR).

Conflict of interest

The authors declare no conflict of interest.

Appendix A. Supplementary material

Supplementary data associated with this article can be found in the online version at doi:10.1016/j.mec.2018.e00082.

References

Altaras, N.E., Cameron, D.C., 2000. Enhanced production of (R)-1,2-propanediol by metabolically engineered *Escherichia coli*. Biotechnol. Prog. 16, 940–946.
Atsumi, S., Hanai, T., Liao, J.C., 2008. Non-fermentative pathways for synthesis of branched-chain higher alcohols as biofuels. Nature 451, 86–89.
Bogorad, I.W., Lin, T.-S., Liao, J.C., 2013. Synthetic non-oxidative glycolysis enables complete carbon conservation. Nature 502, 693–697.
Booth, I.R., et al., 2003. Bacterial production of methylglyoxal: a survival strategy or death by misadventure? Biochem. Soc. Trans. 31, 1406–1408.
Cameron, D.C., Cooney, C.L., 1986. A novel fermentation: the production of R(-)-1,2-propanediol and acetol by Clostridium thermosaccharolyticum. Bio/Technology 4, 651–654.
Campodonico, M.A., Andrews, B.A., Asenjo, J.A., Palsson, B.O., Feist, A.M., 2014. Generation of an atlas for commodity chemical production in *Escherichia coli* and a novel pathway prediction algorithm, GEM-Path. Metab. Eng. 25, 140–158.
Chang, D.-E., Jung, H.-C., Rhee, J.-S., Pan, J.-G., 1999. Homofermentative production of D- or L-lactate in metabolically engineered Escherichia coli RR1. Appl. Environ. Microbiol. 65, 1384–1389.
Chatsurachai, S., Furusawa, C., Shimizu, H., 2012. An in silico platform for the design of heterologous pathways in nonnative metabolite production. BMC Bioinform. 13, 93.
Clomburg, J.M., Gonzalez, R., 2011. Metabolic engineering of Escherichia coli for the production of 1,2-propanediol from glycerol. Biotechnol. Bioeng. 108, 867–879.
Edwards, R.A., Keller, L.H., Schifferli, D.M., 1998. Improved allelic exchange vectors and their use to analyze 987P fimbria gene expression. Gene 207, 149–157.
Elferink, S.J.W.H.O., et al., 2001. Anaerobic conversion of lactic acid to acetic acid and 1,2-propanediol by Lactobacillus buchneri. Appl. Environ. Microbiol. 67, 125–132.
Forkner, M.W.. et al., 2005. Vol. 12 644-682 (John Wiley & Sons, Inc.,
Grabar, T.B., Zhou, S., Shanmugam, K.T., Yomano, L.P., Ingram, L.O., 2006. Methylglyoxal bypass identified as source of chiral contamination in L(+) and D(-)-lactate fermentations by recombinant *Escherichia coli*. Biotechnol. Lett. 28, 1527–1535.
Kramer, L., et al., 2018. Characterization of carboxylic acid reductases for biocatalytic synthesis of industrial chemicals. ChemBioChem 19, 1452–1460.
Lee, J.W., et al., 2012. Systems metabolic engineering of microorganisms for natural and non-natural chemicals. Nat. Chem. Biol. 8, 536–546.
Lennart, E., 1954. Studies in Cellulose Decomposition by an Anaerobic Thermophilic Bacterium and Two Associated Non-Cellulolytic Species. (Viktor Pettersons Bokindustrie Aktiebolag).
Lynch, A.S., Lin, E.C.C., 1996. in Regulation of Gene Expression in Escherichia coli 361-381 (Landes).

Mahadevan, R., Schilling, C.H., 2003. The effects of alternate optimal solutions in constraint-based genome-scale metabolic models. Metab. Eng. 5, 264–276.
Monk, J.M., et al., 2017. iML1515, a knowledgebase that computes Escherichia coli traits. Nat. Biotechnol. 35, 904–908.
Nielsen, J., Keasling, J.D., 2016. Engineering Cellular Metabolism. Cell (Camb., MA, U. S.) 164, 1185–1197.
Niu, W., Guo, J., 2015. Stereospecific microbial conversion of lactic acid into 1,2-propanediol. ACS Synth. Biol. 4, 378–382.
Niu, W., Molefe, M.N., Frost, J.W., 2003. Microbial synthesis of the energetic material precursor 1,2,4-butanetriol. J. Am. Chem. Soc. 125, 12998–12999.
Niu, W., Guo, J., Van Dien, S., 2016. In: Van Dien, S. (Ed.), Metabolic Engineering for Bioprocess Commercialization. Springer International Publishing, Cham, 31–52.
Sambrook, J.F., Russell, D.W., Editors, 2000. Molecular Cloning: A Laboratory Manual third edition.. Cold Spring Harbor Laboratory Press.
Sanchez-Riera, F., Cameron, D.C., Cooney, C.L., 1987. Influence of environmental factors in the production of R(-)–1,2-propanediol by Clostridium thermosaccharolyticum. Biotechnol. Lett. 9, 449–454.
Schellenberger, J., et al., 2011. Quantitative prediction of cellular metabolism with constraint-based models: the COBRA Toolbox v2.0. Nat. Protoc. 6, 1290–1307.
Sharan, S.K., Thomason, L.C., Kuznetsov, S.G., Court, D.L., 2009. Recombineering: a homologous recombination-based method of genetic engineering. Nat. Protoc. 4, 206–223.
Sheldon, R.A., 2014. Green and sustainable manufacture of chemicals from biomass: state of the art. Green. Chem. 16, 950–963.
Shelley, S., 2007. A renewable route to propylene glycol. Chem. Eng. Prog. 103, 6–9.
Totemeyer, S., Booth, N.A., Nichols, W.W., Dunbar, B., Booth, I.R., 1998. From famine to feast: the role of methylglyoxal production in Escherichia coli. Mol. Microbiol. 27, 553–562.
Wang, Y., et al., 2012. Homofermentative production of D-lactic acid from sucrose by a metabolically engineered Escherichia coli. Biotechnol. Lett. 34, 2069–2075.
Weeks, A.M., Chang, M.C.Y., 2011. Constructing de Novo biosynthetic pathways for chemical synthesis inside living cells. Biochemistry 50, 5404–5418.
Yim, H., et al., 2011. Metabolic engineering of Escherichia coli for direct production of 1,4-butanediol. Nat. Chem. Biol. 7, 445–452.
Zhang, Y., Buchholz, F., Muyrers, J.P.P., Stewart, A.F., 1998. A new logic for DNA engineering using recombination in Escherichia coli. Nat. Genet. 20, 123–128.
Zhou, S., Shanmugam, K.T., Ingram, L.O., 2003a. Functional replacement of the Escherichia coli D-(-)-lactate dehydrogenase gene (ldhA) with the L-(+)-lactate dehydrogenase gene (ldhL) from Pediococcus acidilactici. Appl. Environ. Microbiol. 69, 2237–2244.
Zhou, S., Causey, T.B., Hasona, A., Shanmugam, K.T., Ingram, L.O., 2003b. Production of optically pure D-lactic acid in mineral salts medium by metabolically engineered Escherichia coli W3110. Appl. Environ. Microbiol. 69, 399–407.

Metabolic engineering of *Escherichia coli* for the *de novo* stereospecific biosynthesis of 1,2-propanediol through lactic acid

Wei Niu[a]*, Levi Kramer[a], Joshua Mueller[a], Kun Liu[b], Jiantao Guo[b]*

[a] Department of Chemical & Biomolecular Engineering, University of Nebraska-Lincoln, Lincoln, Nebraska, 68588, United States.

[b] Department of Chemistry, University of Nebraska-Lincoln, Lincoln, Nebraska, 68588, United States.

* To whom correspondence should be addressed: wniu2@unl.edu

Table of Contents

Table S1. Primers used in the study.

Primers	Sequences (5' -> 3')
PflB-SacB-F	tcgaagtacgcagtaaataaaaaatccacttaagaaggtaggtgttacatgtagtctgcaaatccttttatg
PflB-SacB-R	gagcctttattgtacgctttttactgtacgatttcagtcaaatctaattatgatctgatccttcaactcag
PflB-F-del	gatatcgcatgcggtaccatgtggctttccggcgagtatatg
PflB-R-del-internal	aggtgttactaattagatttgactgaaatc
PflB-F-del-internal	tctaattagtaacacctaccttcttaag
PflB-R-del	gttggtgtccagacaggtatg
FrdA-SacB-F	accctgaagtacgtggctgtgggataaaaacaatctggaggaatgtcgtg tagtctgcaaatccttttatg
FrdA-SacB-R	cgacttccgggttatagcgcaccacctcaattttcaggtttttcatctca tgatctgatccttcaactcag
FrdA-F-del	gaaacgtgtctcaaacgggac
FrdA-R-del-internal	caggtttttgacattcctccagattgtttttatc
FrdA-F-del-internal	gaatgtcaaaaacctgaaaattgaggtggtg
FrdA-R-internal	catacgctccttcttaccgtg
AldA-SacB-F	aacaatgtattcaccgaaaacaaacatataaatcacaggagtcgcccatg tagtctgcaaatccttttatg
AldA-SacB-R	ctctgacgcgcacaggcggaggaaaaaacctccgcctctttcactcatta tgatctgatccttcaactcag
AldA-F-del	tatgactggggacaatcccgatg
AldA-R-del-internal	ttcactcagggcgactcctgtgatttatatg
AldA-F-del-internal	agtcgccctgagtgaaagaggcggaggtttttc
AldA-R-del	gcacccagtcactggtggatg
MgsA-SacB-F	taagtgcttacagtaatctgtaggaaagttaactacggatgtacattatgtagtctgcaaatccttttatg
MgsA-SacB-R	ggcgagaaaaccgtaagaaacaggtggcgtttgccacctgtgcaatatta tgatctgatccttcaactcag
MgsA-F-del	ctggtggtcagttttaatacccag
MgsA-R-del-internal	ctgtgcaatattaaatgtacatccgtagttaac
MgsA-F-del-internal	gtacatttaatattgcacaggtggcaaacg
MgsA-R-del	ctaaacagcttaaccaatggagac
ArcA-SacB-F	cttttgtacttcctgtttcgatttagttggcaatttaggtagcaaacatgtagtctgcaaatccttttatg
ArcA-SacB-R	aaaacggcgctaaaaagcgccgttttttttgacggtggtaaagccgattatgatctgatccttcaactcag
ArcA-F-del	tcgttagtcaacccggaatcttc

ArcA-R-del-internal	taaagccgagtttgctacctaaattgccaac
ArcA-F-del-internal	gtagcaaactcggctttaccaccgtcaaaaaaaac
ArcA-R-del	taggcaagccatttattgtgattag
ldhA-SacB-F	tatttttagtagcttaaatgtgattcaacatcactggagaaagtcttatgtagtctgcaaatccttttatg
ldhA-SacB-R	ggggattatctgaatcagctcccctggaatgcaggggagcggcaagattatgatctgatccttcaactcag
ldhA-UP-F	ctattttcctgccagtccagctc
ldhA-UP-R-lldh	aagactttctccagtgatgttgaatc
lldh-F	tcactggagaaagtcttatgaagggaatggatattatgtc
lldh-R	caggggagcggcaagatcatttgtcttgtttttcagcaag
ldhA-DOWN-F-lldh	tcttgccgctcccctgcattccag
ldhA-DOWN-R	gaaattgctgcgcgcccagtag

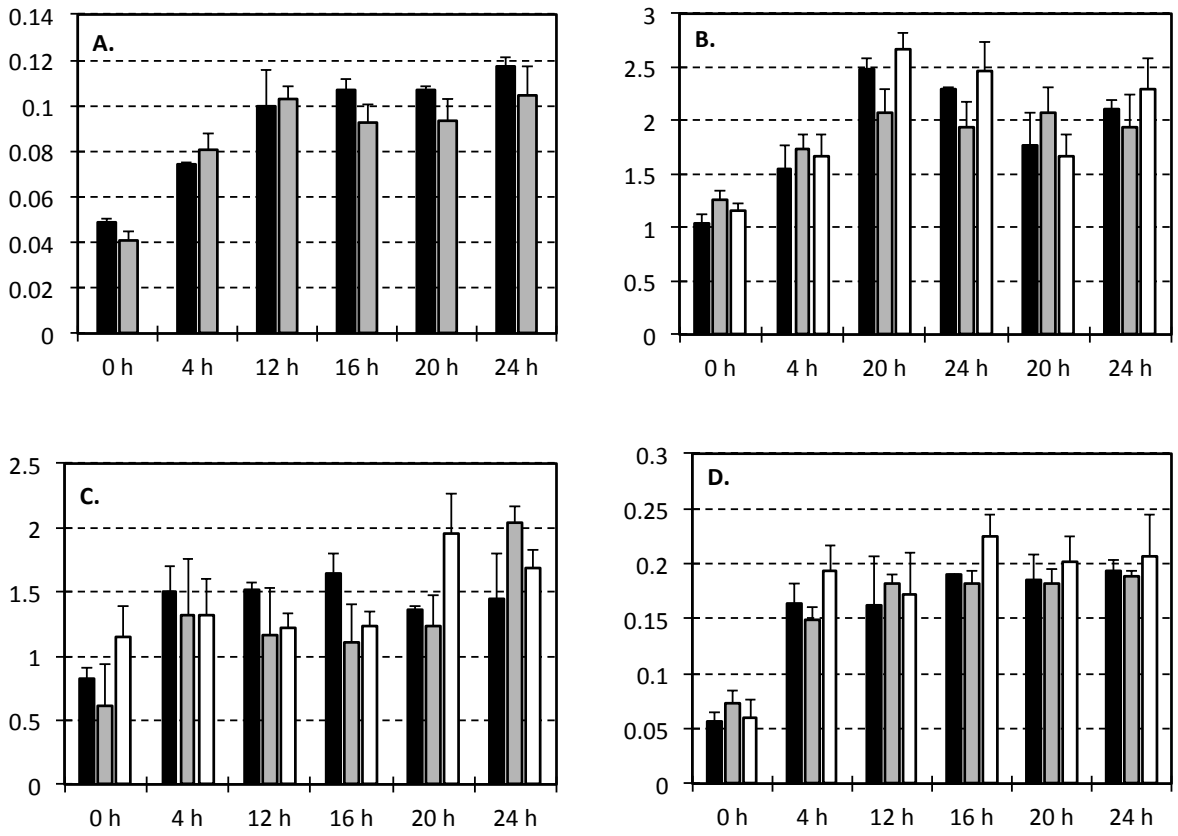

Figure S1. Specific activity of 1,2-PDO pathway enzymes in fed-batch fermentations. All numbers are reported as units of enzyme activity per mg of soluble cell lysate. A. Lactate dehydrogenase (LdhA). One unit of LdhA was defined as the oxidation of 1 µmol of NADH per min at 37 °C; B. Lactoyl-CoA transferase (Pct). One unit of Pct was defined as the formation of 1 µmol of lactoyl-CoA per min at 37 °C; C. Lactoyl-CoA reductase (PduP). One unit of PduP was defined as the oxidation of 1 µmol of NADH per min at 37 °C; D, Lactaldehyde reductase (YahK). One unit of YahK was defined as the oxidation of 1 µmol of NADPH per min at 37 °C. In each plot, filled bars in black, Δ^7/2.094/2.096; filled bars in grey, Δ^8/2.094/2.096; open bars, Δ^8 lldh/2.094/2.096.

Table S2. Cell growth at the aerobic stage of fermentations.

	Δ^7/2.094/2.098	Δ^8/2.094/2.098	Δ^8lldh/2.094/2.098	Δ^8/2.094/2.098	Δ^8lldh/2.094/2.098
time[a]	560 rpm	560 rpm	560 rpm	280 rpm	280 rpm
-8 h	0.33±0.01	0.33±0.02	0.34±0.01	0.32±0.03	0.33±0.01
-2 h	7.1±0.5	6.8±0.7	7.4±0.4	7.1±0.9	7.1±0.4
-1 h	14.7±0.8	14.3±0.6	14.8±0.7	15.0±0.7	16.2±0.6
0 h	23.8±0.4	24.0±0.5	24.7±1.0	23.8±0.3	24.5±0.5

[a] t = -8h, time of inoculation; t = -1 h, time of induction with IPTG; t = 0 h, initiation of the micro-aerobic stage.

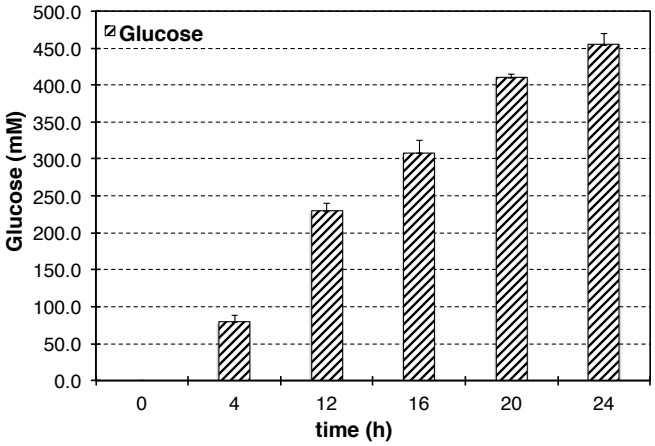

Figure S2. Glucose accumulation by strain Δ^8Ildh/2.094/2.096 (280 rpm stirring rate).